

EFFECT OF INTER-PERIOD CORRELATION IN GROUND MOTION ON RISK EVALUATION FOR PORTFOLIO OF STRUCTURES

Sei'ichiro Fukushima¹

¹ CEO, RKK Consulting Co., Ltd., Tokyo, Japan (fukushima@rkk-c.co.jp)

ABSTRACT

Following Fukushima and Yashiro (2002), the author has conducted probabilistic seismic risk analyses for portfolios of structures situated at different sites. It has been observed that the probable maximum loss (PML) for a portfolio is smaller than the sum of the PMLs of individual structures due to the spatial correlation of ground motion. Similarly, the PML for a portfolio consisting of structures with different natural periods is expected to be smaller than the sum of the individual PMLs, even if they are located at the same site, owing to the inter-period correlation of spectral acceleration. In this study, the author proposes a seismic risk analysis method that incorporates the inter-period correlation of spectral acceleration for a portfolio of structures with varying natural periods, in order to quantify the risk reduction effect through a trial calculation using a model portfolio. The results confirmed that the risk reduction effect increases as the ratio between natural periods becomes larger. Furthermore, as the number of structures in the portfolio increases, the probability of simultaneous damage decreases, leading to a greater overall risk reduction.

INTRODUCTION

The author has previously conducted probabilistic seismic risk assessments targeting multiple buildings located at different sites. In seismic risk assessment, a seismic risk curve, representing the relationship between losses and their corresponding annual exceedance probabilities, is evaluated. The loss corresponding to a given annual exceedance probability is considered PML. The PML obtained for the building portfolio was smaller than the sum of the PMLs evaluated for individual buildings, indicating the risk reduction effect due to the spatial dispersion of the buildings. This risk reduction effect is attributed to the fact that the uncertainty in ground motion intensity is not perfectly correlated between sites. Takada and Shimomura (2003), Hayashi *et al.* (2006), and Park *et al.* (2007) have proposed regression equations for correlation coefficients as a function of inter-site distance.

By the way, a ground motion intensity measure that shows high correlation with the uncertainty of building response is the spectral acceleration at the fundamental period of the target building, which is commonly adopted as the intensity measure in risk assessments. The uncertainty in spectral acceleration is influenced by the inter-period correlation that arises from differences in fundamental periods. Tanaka *et al.* (2008), Inoue (1997), and Baker and Jayaram (2008) have proposed regression equations that describe the inter-period correlation of spectral acceleration uncertainty, demonstrating that the degree of correlation decreases as the difference between fundamental periods increases. In addition, Itoi *et al.* (2015) proposed a regression model for crustal earthquakes that combines inter-site and inter-period correlations, representing the overall correlation as the product of the inter-period correlation and the inter-site correlation expressed as a function of period.

Therefore, similar to the case of buildings located at different sites, when assessing a building portfolio with different fundamental periods, considering the correlation of uncertainties due to period differences is expected to reveal a risk reduction effect. It should be noted that the conventional approach to risk assessment, which uses a single ground motion intensity measure such as peak acceleration or peak

velocity, implicitly assumes perfect correlation in ground motion intensity and does not account for differences in the fundamental periods of buildings.

If such risk reduction through inter-period correlation is indeed feasible, it is expected that more rational planning can be achieved, not only in the design of new building portfolios but also in seismic retrofit strategies, for example, by appropriately selecting brittle and ductile buildings. So, this study focuses on the divergence of buildings' fundamental periods and evaluates the risk reduction effect due to inter-period correlation. While various definitions of risk exist, this study adopts the previously mentioned PML as the measure of risk.

QUANTIFICATION METHOD OF RISK REDUCTION EFFECT

Indicator Representing Risk Reduction Effect

Prior to quantifying the risk reduction effect, the author defines an indicator E to represent the degree of risk reduction, as follows:

$$E(p) = PML_0(p) / \sum_{j=1}^n PML_j(p) \quad (1)$$

where, p is the annual exceedance probability used for PML evaluation, PML_j is the PML of building j , PML_0 is the PML of the building portfolio, and, n is the number of buildings in the portfolio. A smaller value of $E(p)$, as indicated by equation (1), suggests a greater risk reduction effect.

Seismic Risk Assessment Method for Building Portfolios

Overview of the Multi-Event Model

As described in Fukushima and Yashiro (2002), the author has adopted a method based on the *multi-event model* for the probabilistic seismic risk assessment of building portfolios. The multi-event model discretizes the seismic environment surrounding the portfolio into a set of source events and performs statistical processing on the risk evaluation results for each event. This paper also adopts the multi-event model. An overview of the model is presented in Fig. 1.

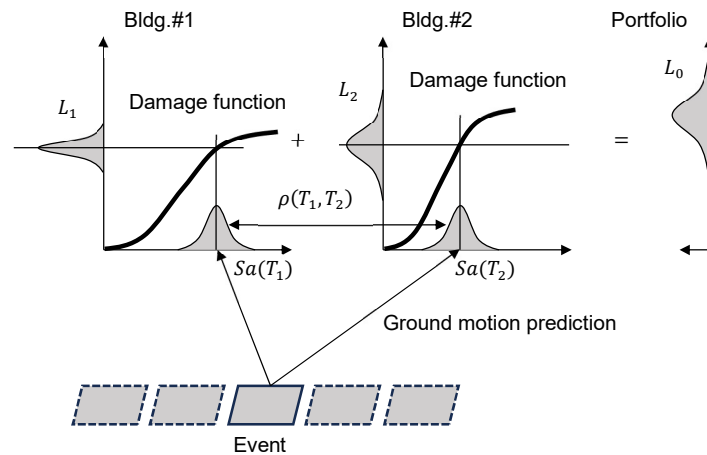


Figure 1. Concept of multi-event model

For simplicity, the figure illustrates the case of two buildings. This study differs from the multi-event model in Fukushima and Yashiro (2002) in two key aspects:

- Different ground motion intensity measures are used for each building, depending on their fundamental period.
- The variability in sampled ground motions considers the correlation.

Procedure and Assumptions for Seismic Risk Curve Evaluation

The procedure for evaluating seismic risk curves using the above multi-event model is illustrated in Fig. 2.

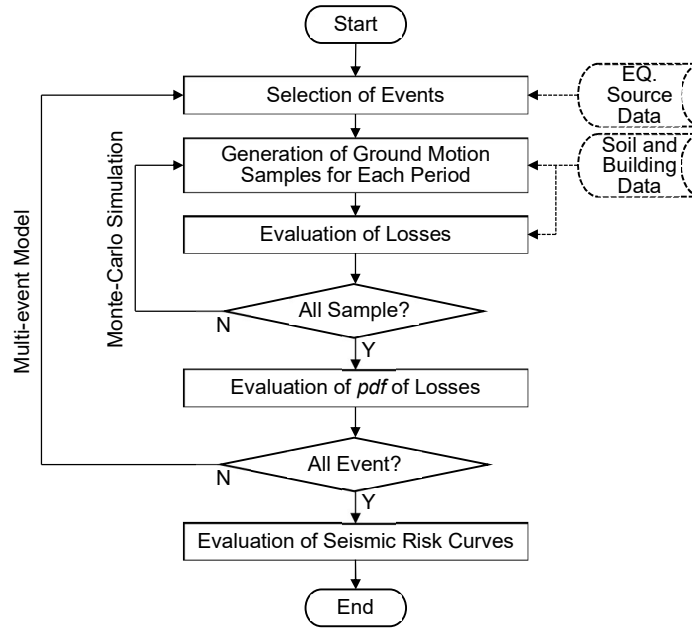


Figure 2. Flowchart to obtain seismic risk curve

a. Event selection

From the set of seismic events defined in the source model, those contributing to the seismic risk of the building portfolio are selected. Each event contains:

- Geometrical parameters: reference point coordinates, depth, strike, dip, fault length, and width
- Seismic activity parameters: annual occurrence rate and magnitude

In this study, the seismic source model from the NIED (2019) is used. Earthquake occurrence is modelled as a Poisson process. It is noted that only events with epicentral distances within 200 km from any building in the portfolio are considered.

b. Generation of ground motion intensity samples for each period

For each building's period, the median and logarithmic standard deviation of ground motion intensity are evaluated. This study adopts the ground motion prediction equation (GMPE) by NIED (2009), GMPE is expressed as follows:

$$\log pre = a_1 M_w + b_1 X - \log(X + d_1 \cdot 10^{0.50 M_w}) + c_1 \quad \text{if, } D \leq 30 \text{ km} \quad (2a)$$

$$\log pre = a_2 M_w + b_2 X - \log(X) + c_2 \quad \text{if, } D > 30 \text{ km} \quad (2b)$$

where, pre is the predicted ground motion intensity at sites with average soil conditions ($V_s = 300$ m/s), taken as 5%-damped spectral acceleration (cm/s^2), M_w is moment magnitude, X is the closest distance to the fault (km), D is source depth (km). a , b , c , and d are regression coefficients depending on the ground motion intensity measure and source depth.

The site amplification factor is calculated based on the average S-wave velocity at each site, obtained from J-SHIS, using an empirical amplification function as follows:

$$\log G = p \log AVS30 + q \quad (3)$$

where, G is the site amplification factor, $AVS30$ is average S-wave velocity up to 30 m depth. p and q are regression coefficients.

The logarithmic standard deviation representing the uncertainty of ground motion intensity is assumed to be 0.2 (base-10 logarithm), regardless of the natural period. Furthermore, samples of ground motion intensity were generated by considering the median and logarithmic standard deviation of the ground motion intensity, as well as the inter-period correlation. The inter-period correlation was calculated using the following equation from Tanaka et al. (2008):

$$\rho(T_1, T_2) = 1 - 0.306 \left| \ln \left(\frac{T_1}{T_2} \right) \right| \quad \text{for } T_1, T_2 \geq 0.1 \text{ s} \quad (4)$$

where, T_1 and T_2 are the natural periods. When either natural period is less than 0.1 s, the correlation coefficient is set to unity. The number of samples generated was set to 200, consistent with the number of Monte Carlo Simulation (MCS) trials.

c. Loss estimation

The loss for each building is evaluated using a damage function that expresses the relationship between ground motion intensity and loss. The total loss of the building portfolio is evaluated as the sum of the individual losses for each building, as shown in Fig. 1.

d. Evaluation of probability density function of loss

The loss samples are statistically processed, and the loss probability variables $L_{j,i}$ for each building and the entire building portfolio are evaluated for each event. Here, the index i represents the event, and j represents the building, with the portfolio set as $j = 0$. The shape of the probability distribution is assumed to follow a log-normal distribution.

e. Evaluation of seismic risk curve

Let the annual occurrence frequency of event i be v_i , and let the loss threshold be t . If the probability of the loss from event i exceeding the threshold for building j is expressed as $p(L_{i,j} > t)$, the annual exceedance frequency $\lambda_j(t)$ for a given threshold t is given by the following equation:

$$\lambda_j(t) = \sum_{i=1}^N (v_i \cdot p(L_{i,j} > t)) \quad (5)$$

where, N is the number of events. Furthermore, assuming the occurrence of events follows a Poisson process, the annual exceedance probability $P_j(t)$ for threshold t is given by:

$$P_j(t) = 1 - \exp(-\lambda_j(t)) \quad (6)$$

The relationship between the threshold t and the annual exceedance probability $P_j(t)$ is expressed as the seismic risk curve.

MODEL BUILDING AND THIR DAMAGE FUNCTION

In this study, buildings located in Tokyo with natural periods of 0.3 s, 1.0 s, and 3.0 s are employed as model buildings. The study site is located at 139.69175° east longitude and 35.689472° north latitude, with an AVS30 value of 261 m/s.

The evaluation method for the damage functions follows Kimura *et al.* (2024). The resulting damage functions are shown in Fig.3.

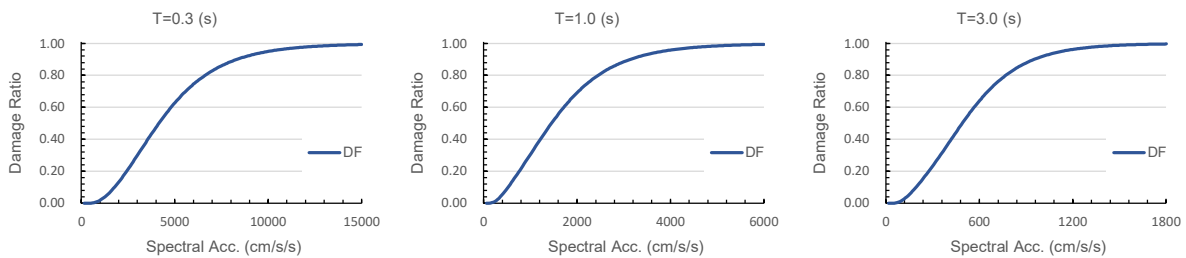


Figure 3. Damage functions of model buildings

SEISMIC RISK ASSESSMENT OF BUILDING PORTFOLIOS

Assumed Building Portfolios

In this study, the replacement cost of each building comprising the portfolio is uniformly set to 100, and seismic risk assessments are conducted for the four types of building portfolios shown in Table 1. The building portfolios are assumed to be located at the site of the Tokyo Metropolitan Government Building, and the site condition is represented by the AVS30 value at that location.

Table 1: Composition of building portfolios

	Building (0.3s)	Building (1.0s)	Building (3.0s)
Portfolio A	○	○	-
Portfolio B	○	-	○
Portfolio C	-	○	○
Portfolio D	○	○	○

Comparison of Seismic Risk Curves

The resulting seismic risk curves are shown in Fig. 4. The upper panel presents the seismic risk curves for individual buildings, where the horizontal axis represents the loss amount and the vertical axis indicates the annual exceedance probability of that loss.

The lower panel replaces the horizontal axis of the left panel with the loss ratio. A comparison of loss ratios at a given annual exceedance probability reveals that, in general, the loss ratio for the building portfolio is smaller than the average loss ratio of individual buildings. This indicates that considering inter-period correlation can lead to risk reduction.

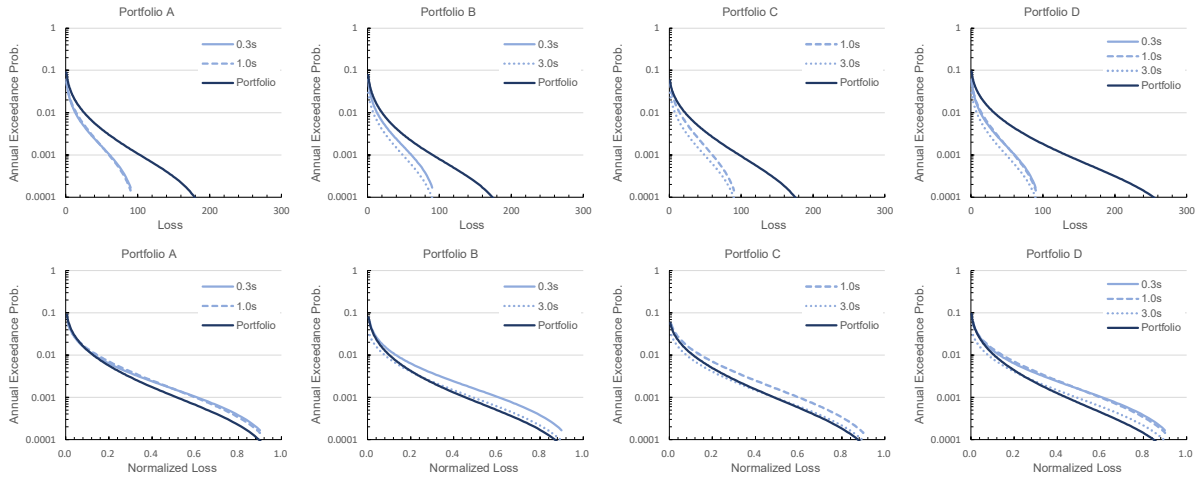


Figure 4. Comparison of seismic risk curve

Comparison of PML and Risk Reduction Effects

As shown in Eqn. (1), in this study, the risk reduction effect is confirmed by the ratio of the portfolio's PML to the sum of the individual buildings' PMLs. PML is typically defined as the loss corresponding to an annual exceedance probability of $1/475$, and this definition is also referenced in this study. The results of the PML calculations for each building portfolio are summarized in Table 2.

Table 2: Comparison of PML at annual exceedance probability of $1/475$

Portfolio	PML at Annual Exceedance Prob. of $1/475$				Portfolio	PML Ratio
	Bldg. (0.3s)	Bldg. (1.0s)	Bldg. (3.0s)	Sum		
Portfolio A	43.04	43.72	-	86.77	72.89	0.840
Portfolio B	43.04	-	32.37	75.42	61.90	0.821
Portfolio C	-	43.72	32.37	76.10	68.31	0.898
Portfolio D	43.04	43.72	32.37	119.14	92.83	0.779

According to the table, the reduction in PML is approximately 10–20%. In the comparison of portfolios A to C, it is observed that the larger the ratio of the natural period, the greater the reduction effect. Furthermore, for portfolios D, where there are more buildings, the reduction effect is higher.

The comparison of the total PML and the portfolio PML for each annual exceedance probability is shown in Fig. 5. The upper panel of the figure shows the stacked PMLs, while the lower panel shows the ratio of the PMLs. Depending on the annual exceedance probability, a reduction in PML is not always observed. However, within the typical range of annual exceedance probabilities ($1/100$ to $1/1000$), the risk reduction effect is evident for all building portfolios. The loss of reduction effect at higher exceedance probabilities is due to the inherently small PML values being compared. This issue, along with an examination of the loss distribution in this range, will be addressed in future studies. On the other hand, at

lower exceedance probabilities, the losses of individual buildings approach their replacement cost, which diminishes the effectiveness of risk diversification and leads to a reduced risk reduction effect. This corresponds to the flattening of the seismic risk curves shown in the upper panel of Fig. 5.

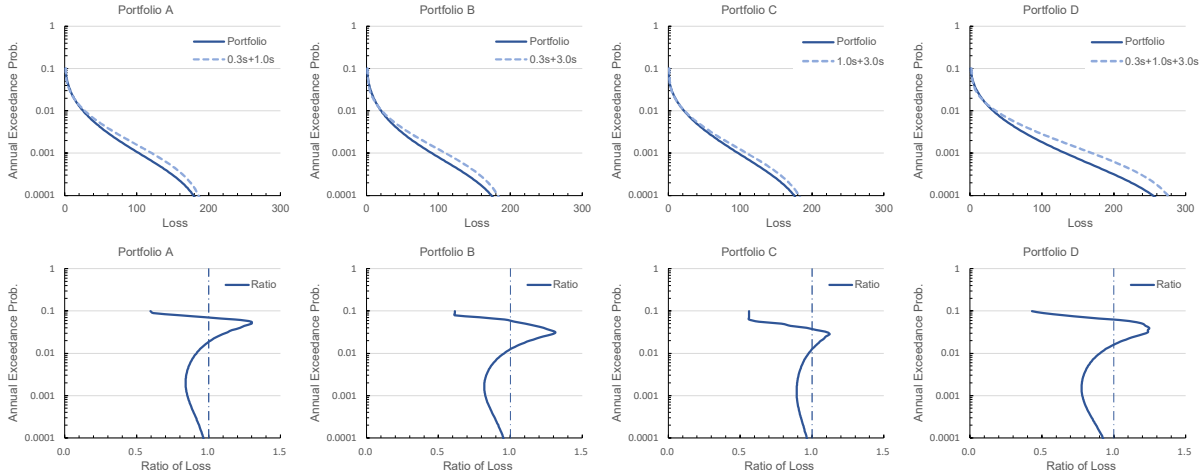


Figure 5. Comparison of PML

Impact of Inter-Period Correlation on the Risk Reduction

The impact of inter-period correlation on risk reduction effects for Building Group D is conducted. Here, the risk reduction effect is quantified under two cases: independent and perfectly correlated. The evaluation results are presented in Fig. 6.

The left panel of the figure shows an overlay of PMLs, while the right panel shows the ratio of PMLs. It can be observed that the smaller the inter-period correlation (i.e., the closer to independence), the lower the PML for the building group, indicating a greater risk reduction effect. In the case of complete correlation, the PML of the building group closely matches the total PML presented in Fig. 5. In principle, these two values should be identical, however, the deviation is minor.

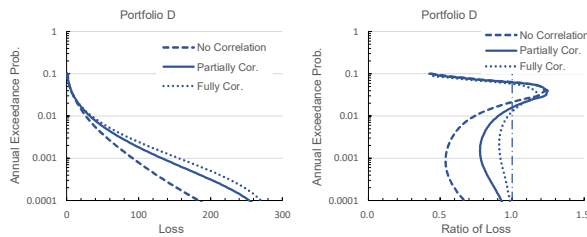


Figure 6. Comparison of PML

COMBINED EFFECT OF INTER-PERIOD AND SPATIAL CORRELATIONS

Approach for Combining Inter-period and Spatial Correlations

The method for combining inter-period and spatial correlations is based on the approach by Itoi *et al.* (2015). In their study, ground motion records from inland earthquakes were used, and the intra-event correlation of ground motion intensity, $\rho_P(\Delta, T_1, T_2)$, was defined by the following equation:

$$\rho_P(\Delta, T_1, T_2) = \rho_P(T_1, T_2) \cdot \exp\left(-\frac{\Delta}{a_P(T_1, T_2)}\right) \quad (6)$$

where, $\rho_P(T_1, T_2)$ represents the inter-period correlation, and Δ is the distance between two sites (km). The parameter $a_P(T_1, T_2)$ is a coefficient that controls the decay of correlation with distance and is determined based on the combination of T_1 and T_2 . For inter-event residuals, a perfect correlation is assumed regardless of the site-to-site distance. As shown in the equation, the correlation $\rho_P(\Delta, T_1, T_2)$ is expressed as the product of the inter-period and spatial correlations.

In this study, assuming continuity with Hayashi *et al.* (2006) and Kimura *et al.* (2024), adopted id Eqn. (7), which combines the inter-period correlation model proposed by Tanaka *et al.* (2008) with the spatial correlation model presented in Hayashi *et al.* (2006).

$$\rho(\Delta, T_1, T_2) = \left[1 - 0.306 \left|\ln\left(\frac{T_1}{T_2}\right)\right|\right] \cdot [\alpha_S + \alpha_P \cdot \exp(-0.042 \cdot \Delta^{1.003})] \quad (7)$$

where, α_S and α_P represent the contributions of inter-event and intra-event variability to the total variability, respectively, and are given as the ratio of the variances of each component (with their sum equal to unity).

Locations of Model Buildings

In this study, the locations of the Tokyo Metropolitan Government Building, the Kanagawa Prefectural Government Building, and the Gumma Prefectural Government Building are used as the building sites. The site locations are shown in Fig. 7. The figure also indicates the coordinates of each site (longitude and latitude) along with the corresponding AVS30 values.

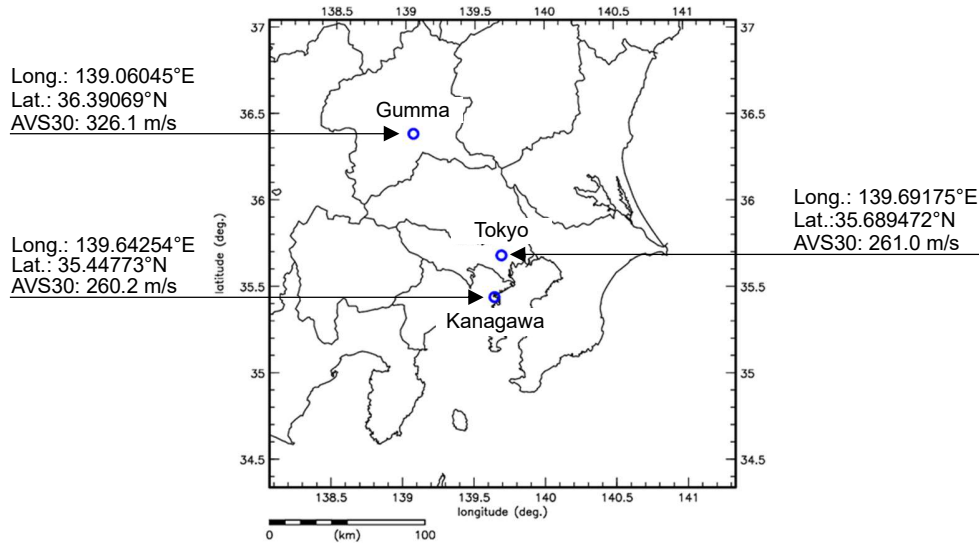


Figure 7. Site locations

The building arrangements considered in this study are summarized in Table 3. In Cases 111, 222, and 333, all three buildings are placed at the same location, resulting in only inter-period correlation being present. In the other cases, buildings with different numbers of stories are arranged at different sites, reflecting both inter-period and spatial correlations.

Table 3: Arrangement case of model buildings

Arrangement Case	Location of Model Building		
	Building (0.3s)	Building (1.0s)	Building (3.0s)
TTT	Tokyo	Tokyo	Tokyo
KKK	Kanagawa	Kanagawa	Kanagawa
GGG	Gumma	Gumma	Gumma
TKG	Tokyo	Kanagawa	Gumma
TGK	Tokyo	Gumma	Kanagawa
KTG	Kanagawa	Tokyo	Gumma
KGT	Kanagawa	Gumma	Tokyo
GTK	Gumma	Tokyo	Kanagawa
GKT	Gumma	Kanagawa	Tokyo

Comparison of PML and Risk Reduction Effect

Table 4 summarizes the sum of the PMLs for individual buildings (Sum) and the PML evaluated for the building portfolio (Portfolio). The table also includes the ratio between the two. In all cases, the ratio is less than unity, indicating that simultaneous occurrence of losses equivalent to the individual building PMLs does not take place.

Table 4: Comparison of PMLs

Arrangement Case	PML		Portfolio/Sum
	Sum	Portfolio	
TTT	119.14	92.83	0.779
KKK	134.44	108.62	0.808
GGG	33.21	27.79	0.837
TKG	106.41	79.22	0.744
TGK	96.47	71.82	0.744
KTG	107.65	81.97	0.761
KGT	98.78	75.94	0.769
GTK	94.55	76.26	0.807
GKT	95.37	78.25	0.820

CONCLUSION

In this study, proposed was a seismic risk analysis method that considers the inter-period correlation of spectral acceleration for a building portfolio consisting of buildings with different natural periods. Through a case study using model building portfolios, quantification of the risk reduction effect was attempted.

As a result of the analysis, it was confirmed that the risk reduction effect increases as the ratio of natural periods becomes larger, that is, as the periods become more distinct. It was shown that the risk reduction effect becomes greater as the number of buildings in the portfolio increases, due to the relatively lower probability of simultaneous damage. A sensitivity analysis was also conducted on the degree of inter-period correlation, and it was confirmed that the smaller the inter-period correlation, the greater the risk reduction effect.

Furthermore, three buildings with different natural periods were placed at multiple sites in the Kanto region to examine the risk reduction effect when both inter-period and spatial correlations are considered. It was confirmed that simultaneously accounting for both correlations results in a greater risk reduction effect.

REFERENCES

- Baker, J.W., Jayaram, N. (2008). “Correlation of Spectral Acceleration Values from NGA Ground Motion Models”, *Earthquake Spectra*, Vol. 24, Issue 1
- Fukushima, S., Yashiro, H. (2002). “Seismic Risk Analysis on Portfolio of Buildings”, *Journal of Architecture and Planning (Transactions of AIJ)*, Vol. 67, No. 552, 169-176. (in Japanese)
- Hayashi, T., Fukushima, S., Yashiro, H. (2006). “Effects of the spatial Correlation between Ground Motion Intensities on Seismic Risk of Portfolio of Buildings”, *Journal of Structural and Construction Engineering (Transactions of AIJ)*, Vol. 71, No. 600, 203-210. (in Japanese)
- Inoue, T. (1997). “Correlation of Response Spectral Values”, *Summaries of technical papers of Annual Meeting Architectural Institute of Japan, B-1, Structures I, Loads, reliability stress analyses foundation structures shell structures, space frames and membrane structures (1997)*, 89-90. (in Japanese)
- Itoi, T., Murakami, M., Sekimura, N. (2015). “Statistical Equations of Response Spectra of Crustal Earthquake for Assessment of Multiple Facilities Seismic Risk”, *Journal of Japan Association for Earthquake Engineering*, Vol. 15, No. 6, 126-141. (in Japanese).
- Kimura, E., Watabe, H., Fukushima, S. (2024). “Quantification of Risk Reduction Effects for Multiple Buildings by Periodic Correlation in Ground Motion”, *Journal of Structural Engineering B*, Vol.70B, 32-39. (in Japanese)
- National Research Institute for Earth Science and Disaster Prevention (2009). “A Study on National Seismic Hazard Maps for Japan”, *Technical Note of the NIED*, No.336. (in Japanese)
- National Research Institute for Earth Science and Disaster Prevention (2019). *J-SHIS, Japan Seismic Hazard Information Station*, (<https://www.j-shis.bosai.go.jp/en/>).
- Park, J., Bazzurro, P., Baker, J.W. (2007). “Modeling Spatial Correlation of Ground Motion Intensity Measures for Regional Seismic Hazard and Portfolio Loss Estimation”, *Applications of Statistics and Probability in Civil Engineering*– Kanda, Takada & Furuta (eds), Taylor & Francis Group, London, ISBN 978-0-415-45211-3.
- Takada, T., Shimomura T. (2003). “Macro-spatial Correlation of Seismic Ground Motion on Strong Motion Records of the 1999 Chi-Chi Earthquake”, *Journal of Structural and Construction Engineering (Transactions of AIJ)*, Vol. 68, No. 565, 41-48. (in Japanese).
- Tanaka, K., Wang, M., Takada, T. (2008), “Covariance structure between spectral Accelerations with Different Periods and its Applications”, *Journal of Structural and Construction Engineering (Transactions of AIJ)*, Vol. 73, No. 632, 1727-1733. (in Japanese).